

# Conformational Studies of the Trimer and Stereoisomeric Tetramers of *n*-Butylsilane

Judith E. Durham

Department of Chemistry, St. Louis University, St. Louis, Missouri 63103

Joyce Y. Corey and William J. Welsh\*

Department of Chemistry, University of Missouri—St. Louis, St. Louis, Missouri 63121

Received March 25, 1991

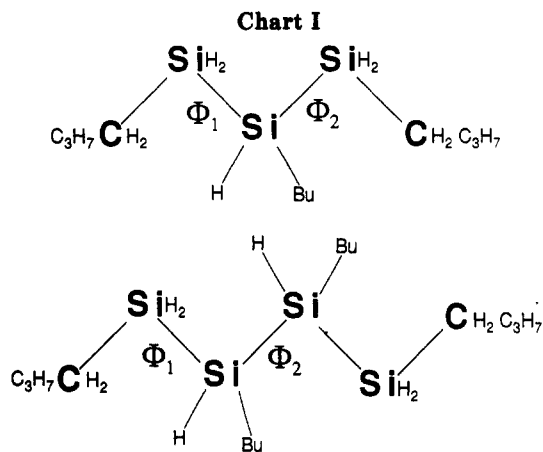
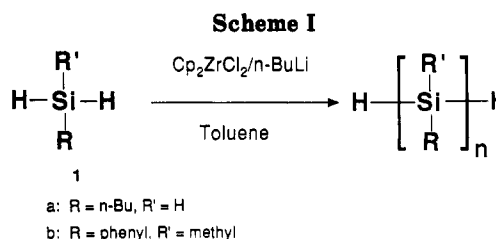
**ABSTRACT:** In order to explain the formation of a nonstatistical distribution of stereoisomers in the transition-metal-catalyzed dehydrogenative coupling of *n*-butylsilane, conformational analyses of the trimer and tetramers of *n*-butylsilane were carried out by using empirical force-field techniques. Structures of the low-energy conformations of the trimer indicate ready access to each heterotopic hydrogen. Conformational energy maps of the stereoisomeric tetramers indicate only slight differences in the size and shape of the low-energy domains. Therefore, the nonstatistical distribution of stereoisomers appears to arise from intermediate transition-metal complexes as opposed to conformational differences in the trimer and/or the tetramers.

## Introduction

There has been considerable interest in recent years in the synthesis and properties of poly(organosilanes)  $[-SiRR']_n$ .<sup>1-3</sup> These organosilane polymers have found commercial applications as UV photoresists in photolithography, as radical photoinitiators, as impregnating agents for strengthening ceramics, and as precursors for silicon carbide fibers. Examples have also shown promise as dopable electrical conductors and semiconductors.

Both homopolymers and copolymers can be prepared by using a Wurtz-type coupling reaction of diorganodichlorosilanes with finely divided sodium metal in an inert solvent, generally at temperatures above the melting point of sodium. However, both yield and molecular weight distribution are particularly sensitive to miniscule changes in the reaction conditions. The search for synthetic methods capable of better control and predictability has focused on the use of transition-metal-catalyzed dehydrogenative coupling of primary and secondary organosilanes  $[RSiH_3]$  and  $[RR'SiH_2]$ .<sup>4</sup> Although the formation of high molecular weight polymers has not yet been realized, there is promise for this method of synthesis.

While investigating the coupling of primary and secondary organosilanes using dichlorozirconocene and *n*-butyllithium as the catalyst precursor, one of us (J.Y.C.) has observed the formation of a nonstatistical distribution of stereoisomers at the tetramer stage of the oligomerization.<sup>5</sup> Both *n*-butylsilane (**1a**)<sup>5a</sup> and methylphenylsilane (**1b**)<sup>5b</sup> have been condensed (Scheme I). Surprisingly, evidence for a nonstatistical distribution of stereoisomers of the tetrasilane was obtained in both cases. Details of the reactions for methylphenylsilane are described in ref 5b but can be summarized as follows. The reactions were performed by using a 2:1 molar ratio of *n*-butyllithium to dichlorozirconocene, 2 mL of toluene for every 1 g of the silane, and a 30:1 to 60:1 molar ratio of the silane to dichlorozirconocene. The reaction of *n*-butylsilane took place at room temperature in 12–24 h, while the reaction of methylphenylsilane took 2–5 days at 90°. Gas chromatography of the product mixture obtained from **1a** showed the presence of two tetramers. The ratio of the two tetramers varied with time (Table I); the isomer that was

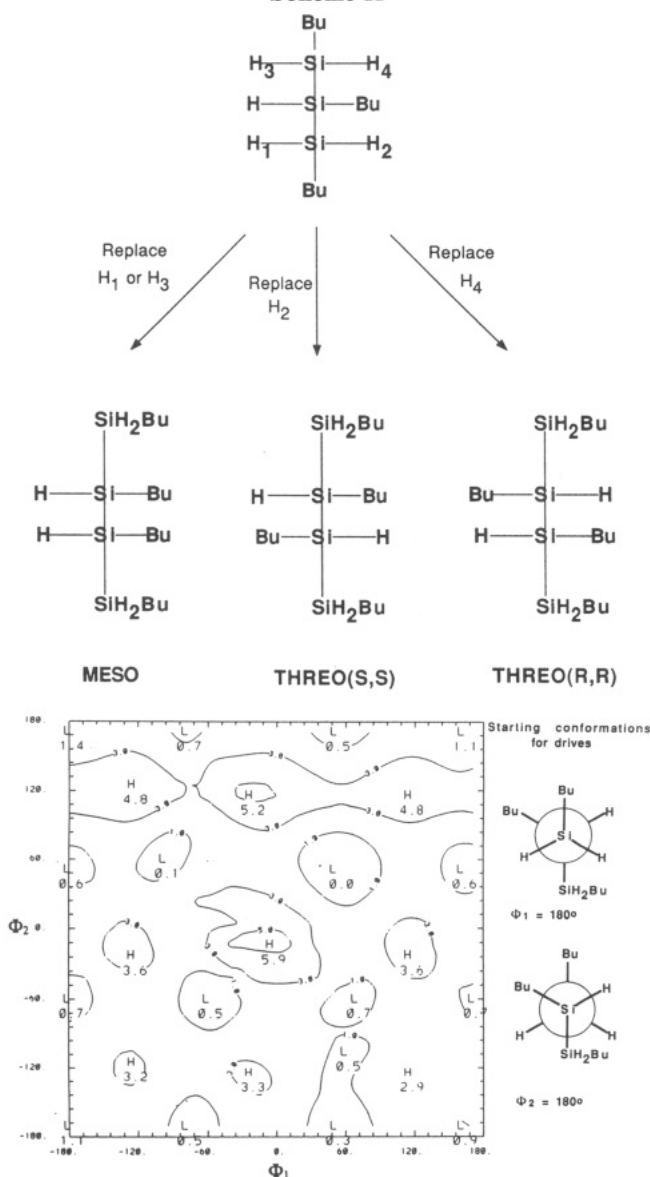


**Table I**  
Gas Chromatography of the *n*-Butylsilane Tetramer

time, h	ratio of diastereomers	time, h	ratio of diastereomers
1	1:8	24	1:0.6
2	1:6	48	1:0.4
19	1:0.8		

formed more quickly also reacted more quickly, presumably forming the pentamer. NMR of the product mixture obtained from **1b** also indicated the formation of a nonstatistical distribution of stereoisomers of the tetramer. The mechanism of the oligomerization is unknown. Since it is possible that the nonstatistical distribution arises from conformational differences, we have initiated computational chemistry studies of the conformations of the tri- and tetrasilanes.

Scheme II

Figure 1. Conformational energy map for  $\text{H}[\text{SiH}(\text{Bu})_3]\text{H}$ .

### Computational Methodology

Conformational analyses of the trimer and tetramers of *n*-butylsilane were carried out by using empirical force-field techniques. Conformational energy calculations were performed by using the MM3 molecular mechanics program<sup>6</sup> with the inclusion of full-geometry optimization. Molecular structures and relative conformational energies were calculated as a function of rotation about two adjacent backbone Si-Si bonds, described by the torsion angles  $\Phi_1$  and  $\Phi_2$  (Chart I). Rotation from  $-180^\circ$  to  $+180^\circ$  (or  $+180^\circ$  to  $-180^\circ$ )<sup>8</sup> was carried out in  $10^\circ$  increments using the "drive" option in MM3. Conformational energy maps were constructed by using NCAR Graphics,<sup>9</sup> and structures of selected minima were visualized using Biosym's Insight II.<sup>10</sup>

### Results and Discussion

Our initial focus has been on the condensation of *n*-butylsilane. Assuming that the oligomerization proceeds by a chain-growth mechanism, the *n*-butylsilane tetramer arises from the achiral trimer. All three silicons in the trimer are prochiral; the hydrogens on the terminal silicons are heterotopic. The stereoisomer formed depends on the

Table II  
Relative Energies for Local Minima of  $\text{H}[\text{SiH}(\text{Bu})_3]\text{H}$ 

$\Phi_1$ , deg	$\Phi_2$ , deg	energy above the global minimum (7.3057 kcal mol <sup>-1</sup> )
50	50	0.0000
-100	60	0.1381
50	180	0.3338
50	-180	0.3341
-60	-60	0.4699
60	-110	0.5077
-80	-170	0.5148
-80	180	0.5247
160	50	0.5913
-180	50	0.6432
-180	-60	0.6533
180	-60	0.6823
160	180	0.9405
160	-180	0.9451
-180	-170	1.1346
-180	180	1.1701

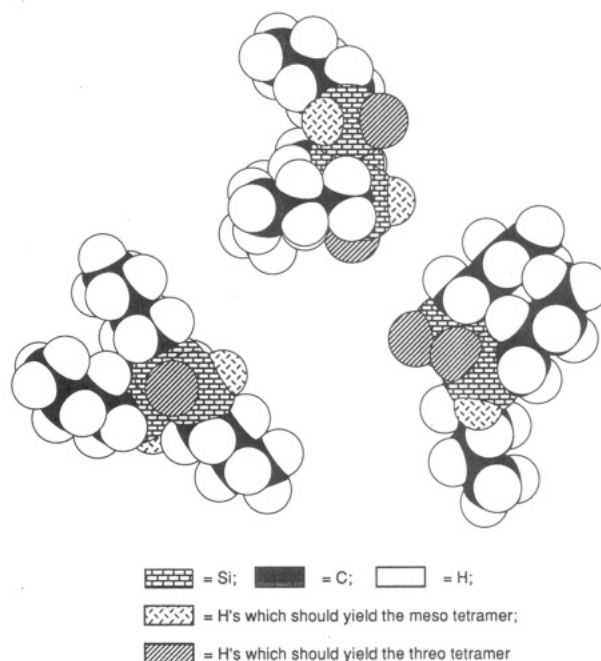


Figure 2. Structures of selected local minima of  $\text{H}[\text{SiH}(\text{Bu})_3]\text{H}$ . [Top:  $\Phi_1 = 50^\circ$ ,  $\Phi_2 = 180^\circ$ ; should yield both the meso and threo tetramers. Left:  $\Phi_1 = 50^\circ$ ,  $\Phi_2 = 50^\circ$ ; should yield the meso tetramer. Right:  $\Phi_1 = -100^\circ$ ,  $\Phi_2 = 60^\circ$ ; should yield the threo tetramer.]

hydrogen replaced in the coupling reaction. Substitution at either hydrogen 1 or 3 gives rise to the meso tetramer, whereas substitution at hydrogen 2 gives the threo-(*S,S*) tetramer and hydrogen 4 gives the threo-(*R,R*) tetramer (Scheme II).

The nonstatistical distribution of the stereoisomers in the formation of the tetramer might arise from one or more of the following:

1. A difference in the availability of the heterotopic hydrogens in the low-energy conformations of the trimer, resulting in the formation of one isomer in preference to the other.
2. A significant difference in the steric energy of the two tetrameric diastereomers, resulting in the formation of one isomer in preference to the other.
3. A significant difference in the steric energy of the possible intermediate zirconium complexes, leading to the formation of one isomer in preference to the other.

The conformational energy map obtained for the trimer is shown in Figure 1. Low-energy domains appear at torsion angles close to  $\pm 60^\circ$  (G) and  $\pm 180^\circ$  (T). Relative

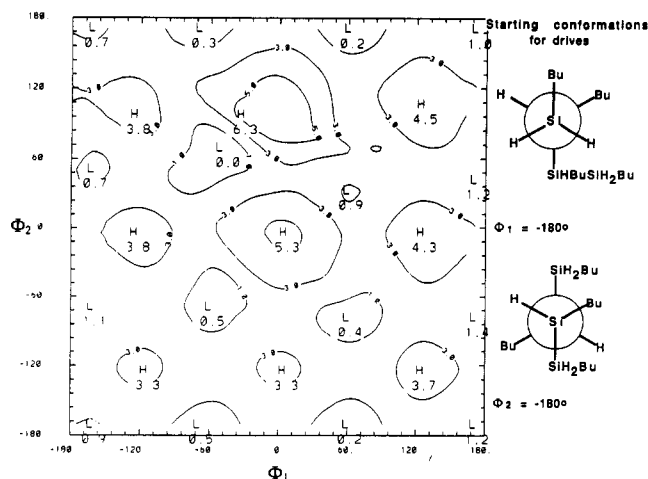


Figure 3. Conformational energy map for *meso*-H[SiHBU]<sub>4</sub>H.

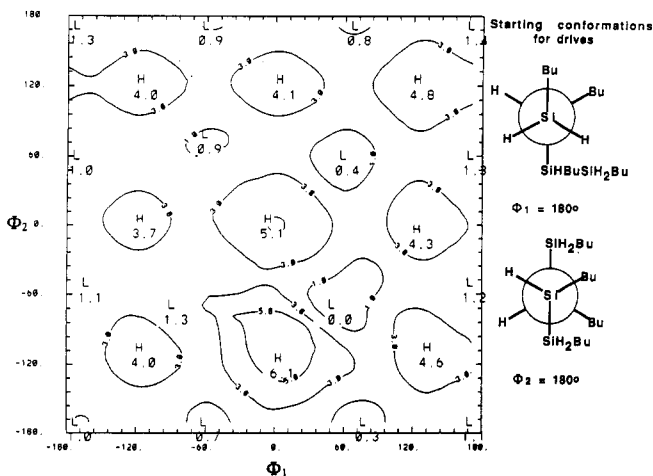


Figure 4. Conformational energy map for *threo*-(*R,R*)-H[SiHBU]<sub>4</sub>H.

energies for minima within each low-energy domain are given in Table II. There appears to be little preference for one rotational state (e.g., G/G, G/T, T/G, or T/T) over another. Figure 2 shows the structures of three of these low-energy conformations.<sup>11</sup> Even though there may be a difference in the availability of hydrogens in a given conformation, one can see that the minima as a whole provide ready access to all four of the heterotopic hydrogens. Thus it appears that the relative availability of the heterotopic hydrogens is not the source of the nonstatistical distribution of the stereoisomers in the formation of the tetramer.

We next turned our attention to the conformational analysis of the stereoisomers of the tetramer. The conformational energy maps for the *meso*, the *threo*-(*R,R*), and the *threo*-(*S,S*) isomers are shown in Figures 3–5. The maps of the *meso* and the *threo*-(*S,S*) isomers are nearly superimposable. There are only slight differences in the size and shape of the low-energy domains. If the conformational energy map of the *threo*-(*R,R*) isomer is rotated 180° around the *Z* axis, it is then nearly superimposable on the map of the *threo*-(*S,S*) isomer. Again, there are only slight differences in the size and shape of the low-energy domains. As with the trimer, low-energy domains for all three stereoisomeric tetramers occur at torsion angles close to ±60° and ±180°, and, again, there is little preference for one rotational state over another. Relative energies for minima within each low-energy domain are given in Tables III–V. As can be seen, there is little difference in the steric energies for the three isomers. Since

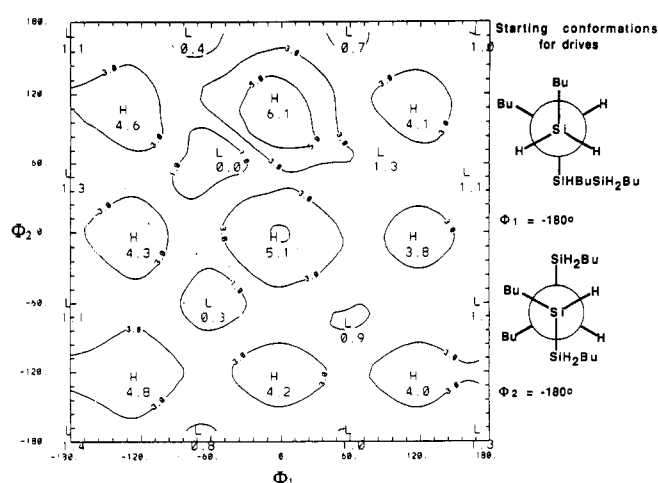


Figure 5. Conformational energy map for *threo*-(*S,S*)-H[SiHBU]<sub>4</sub>H.

Table III  
Relative Energies for Local Minima of *meso*-H[SiHBU]<sub>4</sub>H

Φ <sub>1</sub> , deg	Φ <sub>2</sub> , deg	energy above the global minimum (9.7377 kcal mol <sup>-1</sup> )
-50	70	0.0000
60	180	0.1333
60	-180	0.1599
-70	180	0.2917
60	-80	0.3486
-80	-180	0.4420
-50	-60	0.4700
-160	180	0.7157
-160	50	0.7456
-170	-180	0.8016
180	180	0.8578
180	-180	0.8794
80	70	0.9389
-160	-70	1.0740
180	50	1.0744
180	-70	1.2590

Table IV  
Relative Energies for Local Minima of *threo*-(*R,R*)-H[SiHBU]<sub>4</sub>H

Φ <sub>1</sub> , deg	Φ <sub>2</sub> , deg	energy above the global minimum (9.5347 kcal mol <sup>-1</sup> )
50	-70	0.0000
70	-170	0.3271
60	60	0.3565
80	180	0.5729
-60	-170	0.6847
-60	180	0.7847
-60	70	0.8740
-170	-170	0.9630
-170	60	1.0332
180	-170	1.0400
-160	-50	1.0728
-170	180	1.0978
180	60	1.1328
180	-50	1.2230
-80	-70	1.3108
180	180	1.3436

there is not a significant difference in the steric energies of the stereoisomers, it is unlikely that this is the source of the nonstatistical distribution of the stereoisomers of the tetramer.

Future work will focus on the possible intermediate zirconium complexes. The presence of the large zirconium-containing group should give rise to significant differences in the steric energies of the complexes, leading to the various stereoisomers, and is likely to be the source of the nonstatistical distribution of the *meso* and *threo* isomers.

**Table V**  
Relative Energies for Local Minima of  
*threo*-(*S,S*)-H[SiHBu]<sub>3</sub>H

$\Phi_1$ , deg	$\Phi_2$ , deg	energy above the global minimum (9.5193 kcal mol <sup>-1</sup> )
-50	70	0.0000
-60	-60	0.3381
-70	170	0.3564
-70	-180	0.6092
60	170	0.6913
60	-180	0.8105
60	-80	0.8866
170	170	0.9733
170	-60	1.0501
-180	170	1.0648
170	-180	1.1131
170	50	1.1187
-180	-60	1.1412
-180	50	1.2700
-180	-180	1.2939
90	70	1.3133

## Conclusions

1. Since there appears to be equal accessibility to all heterotopic hydrogens in the *n*-butylsilane trimer, the availability of specific hydrogens is unlikely to cause one stereoisomer to be formed in preference to the other.

2. Since the low-energy domains of the stereoisomeric tetramers of *n*-butylsilane are nearly identical in size and shape and have approximately the same steric energies, differences in the stereoisomers themselves are not responsible for the nonstatistical distribution observed.

**Acknowledgment.** This research was funded by grants to J.Y.C. and W.J.W. from the donors of the Petroleum

Research Fund, administered by the American Chemical Society. Drs. Durham and Welsh are particularly grateful to the donors of the Petroleum Research Fund for a Summer Research Fellowship to support Dr. Durham.

## References and Notes

- (1) West, R. J. *J. Organomet. Chem.* **1986**, *300*, 327.
- (2) Harrah, L. A.; Zeigler, J. M. *Macromolecules* **1987**, *20*, 2039.
- (3) For recent reviews, see: (a) Zeigler, J. M. *Synth. Met.* **1989**, *28*, C581. (b) Miller, R. D.; Michl, J. *Chem. Rev.* **1989**, *89*, 1359.
- (4) Corey, J. Y. In *Dehydrogenative Coupling Reactions of Organosilanes. Advances in Silicon Chemistry*; Larson, G., Ed.; JAI Press: Greenwich, CT, 1991; Vol. 1, pp 327-386 and references cited therein.
- (5) (a) Zhu, X.-H.; Corey, J. Y., unpublished results. (b) Corey, J. Y.; Zhu, X.-H.; Bedard, T. C.; Lange, L. D. *Organometallics* **1991**, *10*, 924.
- (6) (a) Allinger, N. L.; Young, H. Y.; Lii, J. *J. Am. Chem. Soc.* **1989**, *111*, 8551. (b) Lii, J.; Allinger, N. L. *J. Am. Chem. Soc.* **1989**, *111*, 8566. (c) Lii, J.; Allinger, N. L. *J. Am. Chem. Soc.* **1989**, *111*, 8576. (d) MM3 is available from the Technical Utilization Corp., 235 Glen Village Court, Powell, OH 43065.
- (7)  $\Phi = \pm 180^\circ$  corresponds to the *trans* (or *anti*) conformation whereas  $0^\circ$  corresponds to the eclipsed conformation [see Figures 1 and 3-5 for the Newman projections corresponding to  $\pm 180^\circ$ ].
- (8) Due to the Si-Si bond lengths, the backbones of polysilanes are much more flexible than those of the corresponding carbon chains. As a result, the side chains have a tendency to twist out of the normal all-*trans* state and become lodged in higher energy conformations, complicating the conformational energy maps. We have found that running the "drive" in MM3 counterclockwise often avoids or minimizes this problem.
- (9) NCAR Graphics is available from the National Center for Atmospheric Research, Scientific Computing Division, P.O. Box 3000, Boulder, CO 80307.
- (10) Insight II is available from Biosym Technologies, Inc., 10065 Barnes Canyon Road, San Diego, CA 92121.
- (11) The structures shown in Figure 2 were drawn by using Chem3D Plus, which is available from Cambridge Scientific Computing, Inc., 875 Massachusetts Ave., Suite 61, Cambridge, MA 02139.